Anti-HCV and Zika activities of ribavirin C-nucleosides analogues

Simon Gonzalez, Gabriela Brzuska, Abdelhakim Ouarti, Florian Gallier, Carmen Solarte, Angélique Ferry, Jacques Uziel, Ewelina Krol, Nadège Lubin-Germain

Anti-HCV and Zika activities of Ribavirin *C*-Nucleosides analogues

Simon Gonzalez,[aξ] Gabriela Brzuska,[bξ] Abdelhakim Ouarti,[a] Florian Gallier,[a] Carmen Solarte,[a] Angélique Ferry,[a] Jacques Uziel,[a] Ewelina Krol,[b]* Nadège Lubin-Germain[a]*

[a] CY Cergy Paris Université, CNRS, BioCIS, 95000, Cergy Pontoise, France, Université Paris-Saclay, CNRS, BioCIS, 92290, Châtenay-Malabry, France

[b] Department of Recombinant Vaccines, Intercollegiate Faculty of Biotechnology, University of Gdansk and Medical University of Gdansk, Abrahama 58, 80-307 Gdansk, Poland

[ξ] Authors with equally contribution

*Corresponding author: nadege.lubin-germain@cyu.fr, ewelina.krol@biotech.ug.edu.pl

ABSTRACT

Ribavirin is an unnatural nucleoside exhibiting broad spectrum of antiviral and antitumor activities, still very widely studied particularly in a repositioning approach. *C*-triazolyl nucleoside analogues of ribavirin have been synthesized, as well as prodrugs and glycosylated or peptide conjugates to allow a better activity by vectorization into the liver or by facilitating uptake into the cells. The antiviral properties of all synthesized compounds have been evaluated *in vitro* against two important human viral pathogens belonging to the *Flaviviridae* family: hepatitis C virus (HCV) and Zika virus (ZIKV). There are no therapeutic options for Zika virus, whereas those available for HCV can be still improved. Our results indicated that compound **2** carrying an *N*-hydroxy carboxamide function exhibits the most inhibitory activities against both viruses. This compound moderately inhibited the propagation of HCV with an IC_{50} value of 49.1 µM and Zika virus with an IC_{50} of 33.2 µM comparable to ribavirin in the Vero cell line. The results suggest that compound **2** and its new derivatives may be candidates for further development of new anti-HCV and anti-ZIKV antiviral drugs.

KEYWORDS

C-nucleoside, antiviral activities, ribavirin, Dengue, Hepatitis C, Zika virus

1. Introduction

The discovery of new biologically active compounds is a highly risky, expensive, and time-consuming process. In this context, the approach consisting of developing drugs, already approved, for unexplored therapeutic properties is particularly interesting. In the context of the repurposing approach,[1] ribavirin (**RBV**) is experiencing a renewed interest in the field of oncology on various cancers such as leukemias (Acute Lymphocytic Leukemia ALL,[2] Acute Myeloid Leukemia AML,[3] Chronic Myeloid Leukemia CML[4]), lymphoma, carcinomas (HNSCC, hepatocarcinoma) and breast cancer.[5] These studies show that **RBV** is, at the very least, a potentiator of activity and allows the doses of the cytotoxic agent to be reduced, without causing known undesirable effects, such as anemia. As the result, ribavirin is currently subjected to around 170 clinical trials.[6] **RBV** is also in clinical development against viruses causing haemorrhagic fevers, in particular against two viral infections caused by the Lassa virus (phase 2) and the Crimean-Congo virus (phase 2) in Europe, or respiratory deficiencies elicited by SARS–CoV, MERS-CoV or SARS-CoV-2.[7] This last study highlighted the salient role of small drugs and their repurposing in the emergency of viral pandemic.

Taking into consideration the potential of ribavirin despite its side effects, we turned to the synthesis of *C*-nucleoside analogues of **RBV** and their evaluation for anti-tumor activities. We have recently published the first work on ovarian cancer, and we have shown that compound **1** (**SRO-91**), a *C*-ribosyltriazole (Figure 1) has the capacity to put ovarian cancer cells in quiescence and even to induce selectively their apoptosis.[8] We then investigated other anti-tumor activities by testing **SRO-91** on other cancer cell lines. We have shown that it exhibits activities in a micro-molar range on melanomas, epidermoid carcinomas and gliomas.[9]

We continued then the studies on the antiviral activities of these *C*-nucleoside analogues of **RBV**. Indeed, **RBV** is well-known for its potential against RSV (Respiratory Syncytial Virus) infection and against some RNA viruses belonging to the *Flaviviridae* viral family.[10] **RBV** was first developed in combination with interferon and constituted during a long time the only efficient anti-hepatitis C virus (HCV) treatment despite of numerous side effects. Recently, several compounds proved to be active against emerging viruses and one of them, Remdesivir is the first *C*-nucleoside to be approved for clinical use [11] (Figure 1).

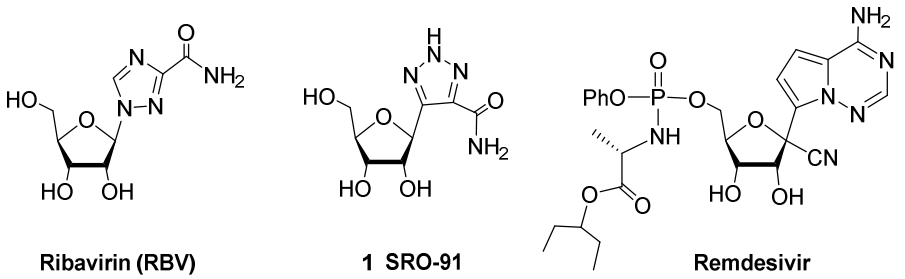

Figure 1. Remdesivir, **RBV** and its analogue **SRO-91**.

The potential of *C*-nucleosides has been recently highlighted by De Clercq *et al.*,[12] partly explained by the reduced sensitivity of *C*-nucleosides to enzymatic degradation, in particular to the PNP (purine nucleoside phosphorylase) due to the carbon-carbon glycosidic bond.

Regarding the urgent need to find new treatments or to potentiate direct antiviral agents (DAA), and considering the potential as pharmacophore of triazole rings,[13] our research focuses on the **SRO-91** analogues and on the investigation of their antiviral activities. The interest of the *C*-ribosyltriazole family has recently been highlighted by the synthesis of the C1'-CN-SRO-91 derivative,[14] carrying a modification of interest recently described for the inhibition of the viral RNA dependent RNA polymerase (RdRp).[15]

After re-examining the access to ribosyltriazoles, we decided to apply a pharmacomodulation approach and on the other hand, to explore the possibility of improving activities by offering prodrugs (Figure 2).

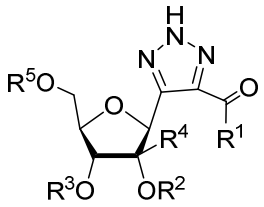

Figure 2. Synthesized compounds **1-15**.

In this study, all of the synthesized compounds have been evaluated for antiviral activities against two viruses belonging to the *Flaviviridae* family: HCV and Zika virus (ZIKV). HCV is a positive-stranded RNA virus which is the major cause of chronic liver diseases, like cirrhosis and liver carcinoma, while Zika virus transmitted by *Aedes* mosquitos is responsible for serious

clinical complications *e.g.*, Guillain Barré syndrome and microcephaly in new-borns.[16,17] The current drug combinations for HCV are well tolerated, however due to extremely high costs, their use is still limited. For Zika virus no drugs have been approved for clinical use. Thus, the development of new anti-HCV and anti-ZIKV compounds is still needed.

2. Results

2.1.Chemistry

We prepared 11 compounds (**1**-**11**), most of which have already been synthesized presenting different modifications onto the carboxamide group[18] or a quaternization of C2' nucleoside position[19] for improving interactions with the unknown target. In a second approach, we also prepared 4 other compounds (**12-15**) as prodrugs presenting an additional group at position 5' (Figure 3).

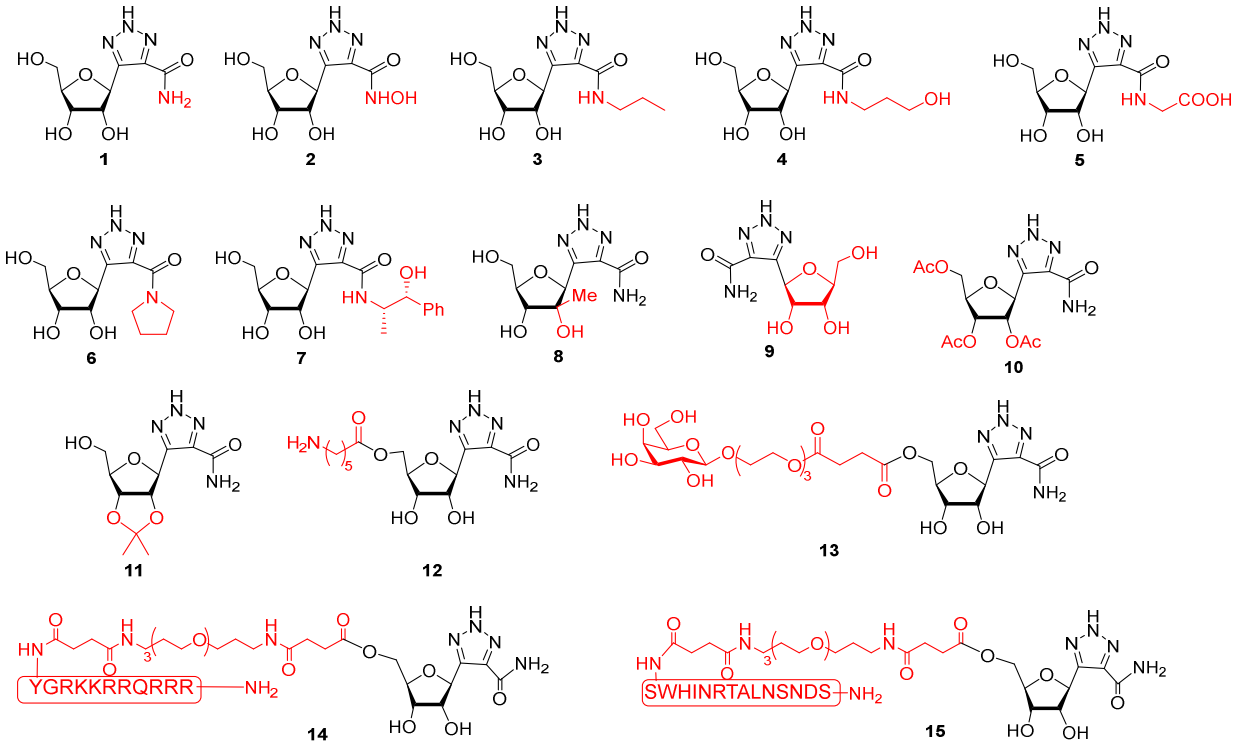

Figure 3. Chemical structure of the 15 compounds.

Compound **1** was previously described[9,20,21] but we re-examined a direct route using trimethylsilylazide for the Huisgen cycloaddition, avoiding by this way the problematic

deprotection of the triazole heterocycle. The synthesis started from compound **16,** obtained by the alkynyl glycosylation mediated by indium, the latter is engaged in the cycloaddition in the presence of $TMSN_3$ in a 9/1 DMF/EtOH mixture for 30 minutes at 120°C (Scheme 1). Different conditions were attempted, but the best results were obtained by using microwave activation which allowed isolation of the cycloadduct **17** in a moderate 59% yield. The latter was used in an aminolysis reaction in the presence of aqueous ammonia in dioxane by heating for two days, to get the carboxamide **1** in 74% yield. Finally, the compound **1** (**SRO-91**) was obtained after deprotection of the isopropylidene group as previously described.

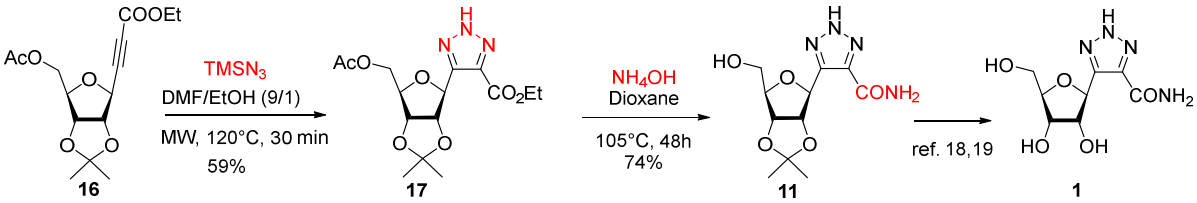

Scheme 1. Synthesis of compound **1** using $TMSN_3$.

Compound **1** was thus produced with an overall yield of 44%. Compared to the previous synthesis,[9,20,21] we improved the access to such ribosyltriazoles and we simplified the synthesis by avoiding the triazole deprotection steps (Benzyl, POM, SEM). Concerning the compounds **2-7**, **11** on one hand and the compound **8** on the other hand, they were already described in the previous papers using the benzyl azide pathway.[18,19] Their design is based on their ability to establish hydrogen bonds like **RBV** and **SRO-91,** possibly with amino acids further away in the target, reducing the solubility in water.

In addition, as **RBV** had shown interesting activities as its enantiomer [22,23] or its acetylated form,[24] therefore we explored these two possibilities in the case of **SRO-91**. Thus, the compound **9** was obtained starting from L-ribose, *via* synthetic route using benzyl azide,[18] with an overall yield of 13%. We have also performed the acetylation reaction (pyridine, Ac_2O) of compound **1** and obtained the peracetylated derivative **10** in a good yield (94%).

Next, we were interested in the synthesis of prodrugs of compound **1**, structurally close to **RBV**. For that, we have followed several approaches by changing the physical-chemical properties and the bioavailability, by increasing interactions with membranes or with possible

receptors. Firstly, we changed the lipophilic properties of compound **1** by adding a hydrocarbon chain at position 5'. The synthesis started with protection of the amine group of 6-amino hexanoic acid **18** leading to compound **19** (Scheme 2). The latter was engaged in the coupling reaction with compound **20**.[18,19] The ester **21** was obtained in a very good yield (81%) and was subjected to hydrogenolysis to remove all protecting groups. This reaction gave compound **12** in moderate yield (40%).

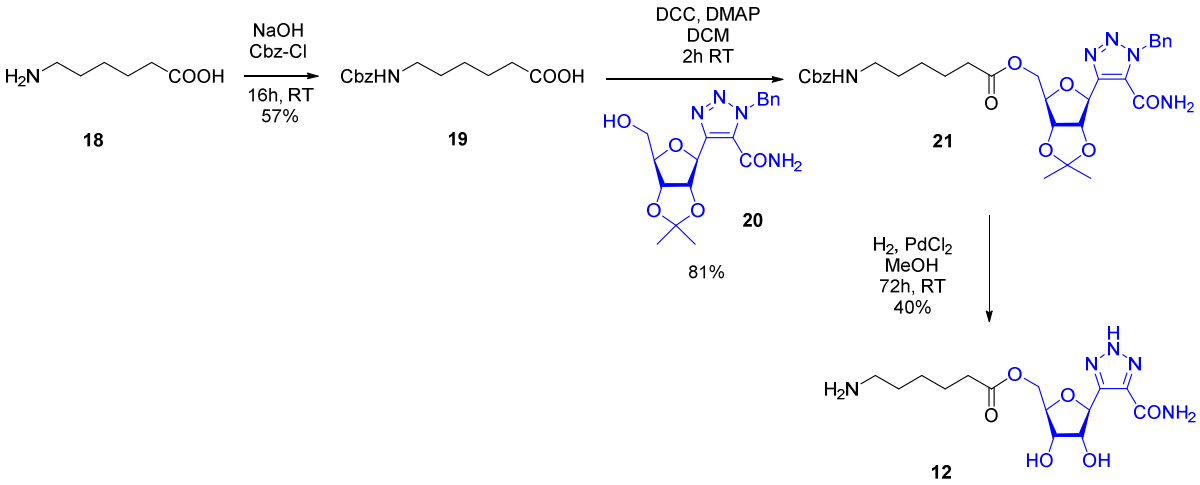

Scheme 2. Synthesis of compound **12**.

Additionally, we anticipated that the interaction with cell membranes could improve the antiviral activity. Actually, we were guided by already published results concerning antiviral activities of HCV fusion peptides[25] and by our recent work on membranotropic properties of HCV and HIV peptides showing a capacity to interact with membranes.[26] We made the hypothesis that the HCV fusion and the HIV-TAT peptides[27] could facilitate the uptake of the drug. Peptides **14** and **15,** which are compound **1** conjugates, were coupled with compound **23** previously synthesized in two steps from compound **20**. In order to prevent perturbations of the peptides' membrane interaction we chose to incorporate a pegylated linker (TTDS) between the nucleoside **1** and the peptide. Additionally, this yielded an ester linkage, prone to enzymatic cleavage, allowing the release of compound **1** in the cellular media. The amine function of the TTDS motif reacted with the carboxylic acid function of compound **23** in the presence of TBTU and NMM in DMF (Scheme 3). Final deprotection with an acidic TFA solution not only cleaved the permanent protective groups and the nucleoside isopropylidene, but also separated the peptide from the

resin. The two peptidyl-nucleoside conjugates **14** and **15** were obtained with purity greater than 95% and a yield of 55 and 12% respectively.

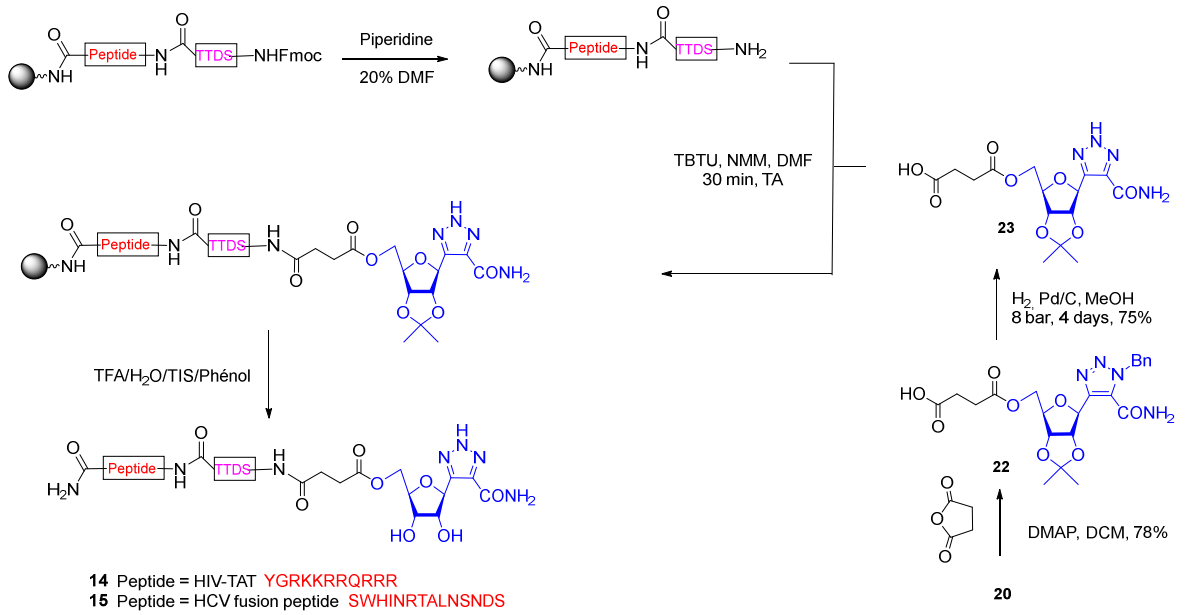

Scheme 3. Synthesis of compounds **14** and **15**.

Finally, we decided to introduce a galactosyl group at the 5' position of the ribosyl moiety with the aim to improve different interactions. Firstly, we considered interactions with receptors such as asialoglycoprotein receptor (ASGP-R) overexpressed at the surface of hepatic cells. Even if the receptor is a tri-antenary galectin, we hypothesized that the presence of one galactosyl residue could help to establish a selective uptake by hepatocytes. As depicted in Scheme 4, compound **13** was obtained by coupling between the protected nucleoside **20**[18] and the galactoside **29**.

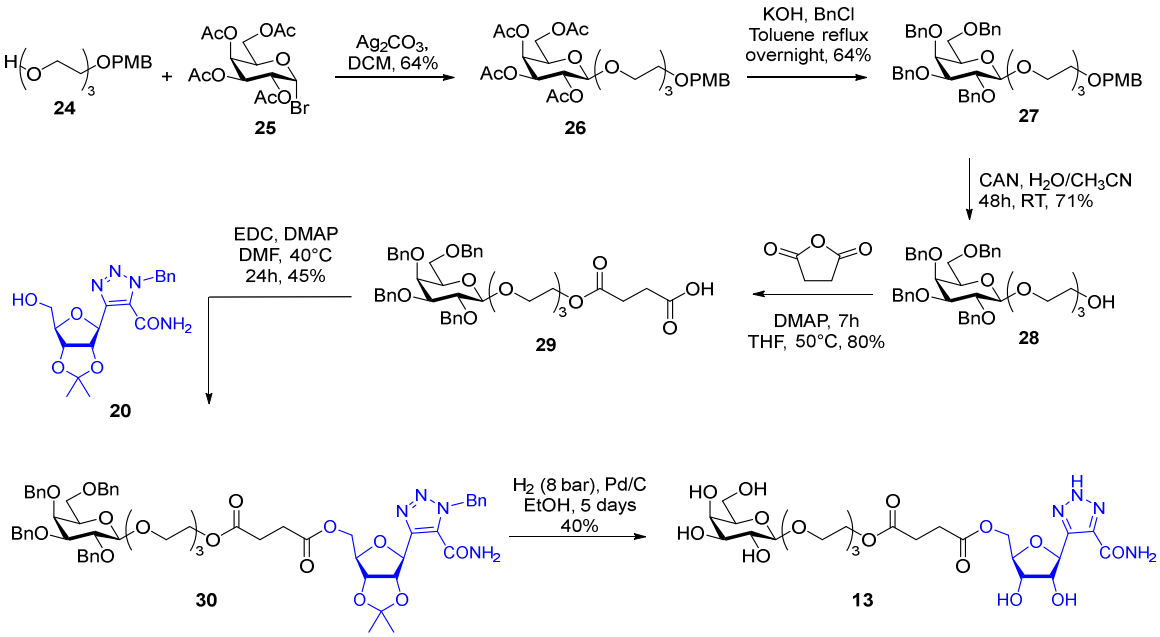

Scheme 4. Synthesis of compound **13.**

The latter was previously prepared by galactosylation (Ag_2CO_3, DCM, 64% yield) in the presence of the *per*-acetylgalactosyl bromide **25**. We exchanged the protecting group in the presence of KOH and benzylchloride (**27**, 64% yield) and applied the deprotection of the PMB protecting group in the presence of CAN reagent in aqueous media. After 48h, we obtained the alcohol **28** (71% yield). This was finally functionalized by reacting with succinic anhydride in tetrahydrofurane. The galactoside **29,** obtained in a satisfying yield (66% yield), was coupled with the nucleoside **20** affording the Galactosyl-TEG-SRO **30** in a modest yield (45%) in the presence of EDC as a coupling agent.[18] Finally, complete deprotection under pressure of hydrogen with Pd/C provided the galactosyl-nucleoside **13** (40% yield).

Having in hand a set of 15 compounds with structural and physicochemical variability, we have undertaken to evaluate their antiviral activities on Zika and hepatitis C viruses.

2.2. Biology

2.2.1 Antiviral activity of *C*-nucleoside analogues of ribavirin against hepatitis C virus

Firstly, we evaluated the activities of synthesized *C*-nucleoside analogues of **RBV** against hepatitis C virus. For this purpose, Huh 7.5 cell culture-derived HCV (HCVcc), genotype 2a

(JFH-AM71) - a high-titer producing virus - was used. The antiviral activity was analyzed using a reporter assay based on Huh7-J20 cell line.[28] It is a derivative of human hepatocellular carcinoma cell line, which stably expresses the fusion protein - EGFP fused in-frame to the secreted alkaline phosphatase (SEAP) via a recognition sequence of the viral NS3/4A serine protease. After HCVcc virus infection, SEAP is cleaved by the protease resulting in its secretion into the culture medium. The level of SEAP directly correlates with the level of HCVcc replication; therefore, this reporter assay was chosen for the antiviral activity evaluation. Firstly, the cytotoxicity of synthesized compounds was assessed. A MTS-based method was used to analyse the viability of non-infected cells after treatment with a range of compound doses and to estimate the half-maximal cytotoxic concentration values (CC_{50}) (Table 1). Compounds **1-13** showed low to moderate cytotoxicities; for some of the compounds, the cytotoxicity was similar to that caused by **RBV** (CC_{50} 1019.17 μM). Within this group of compounds, compound **5** was the most toxic (CC_{50} 363.78 μM), however the CC_{50} value was still only 3 times lower than for **RBV**. Compounds **14** and **15** were analysed in other range of concentrations due to the high molecular mass. CC_{50} values were estimated on the level of 0.1 and 0.08 μM, respectively.

Table 1. The cytotoxicity of *C*-nucleoside analogues of **RBV** in Huh 7-J20 cell line.

COMPOUNDS	**CC_{50} [μM]^{A}**	**COMPOUNDS**	**CC_{50}[μM]^{A}**
RBV	1019.7	**8**	1335.75
1	1079.3	**9**	807.7
2	823.13	**10**	569.7
3	730.45	**11**	904.4
4	911.79	**12**	561.6
5	363.78	**13**	648.78
6	620.6	**14**	0.1
7	709.4	**15**	0.08

[a] Concentration of the compound causing reduction in cell viability by 50%

Further, the preliminary screening of the antiviral activity of synthesized compounds and **RBV** as a positive control was performed. Huh 7-J20 cells were treated with the highest nontoxic

concentration (<15% cytotoxicity): 100 µM for ribavirin and compounds **1-13**; 0,045 µM for compound **14-15**, respectively. Overnight grown Huh 7-J20 cells were infected with HCVcc virus (JFH-AM71, multiplicity of infection (MOI) 0,01) and treated with synthesized compounds or DMSO (negative control) for 3 days, then the cell culture medium was collected. The SEAP assay was used for the assessment of HCVcc replication inhibition (Figure 4). The results indicate that six compounds (**1-4**, **14-15**) demonstrated moderate antiviral activities (µM range) as compared to **RBV** which showed 80% inhibition of HCVcc replication. The highest activity was observed for compounds **1** and **2** (60 and 67% inhibition of HCVcc replication, respectively). Compounds **3**, **4**, **14** and **15** were less potent and exhibited around 45-50% inhibition of HCVcc replication. Thus, based on the obtained results only compounds **1-4** were chosen for further evaluation.

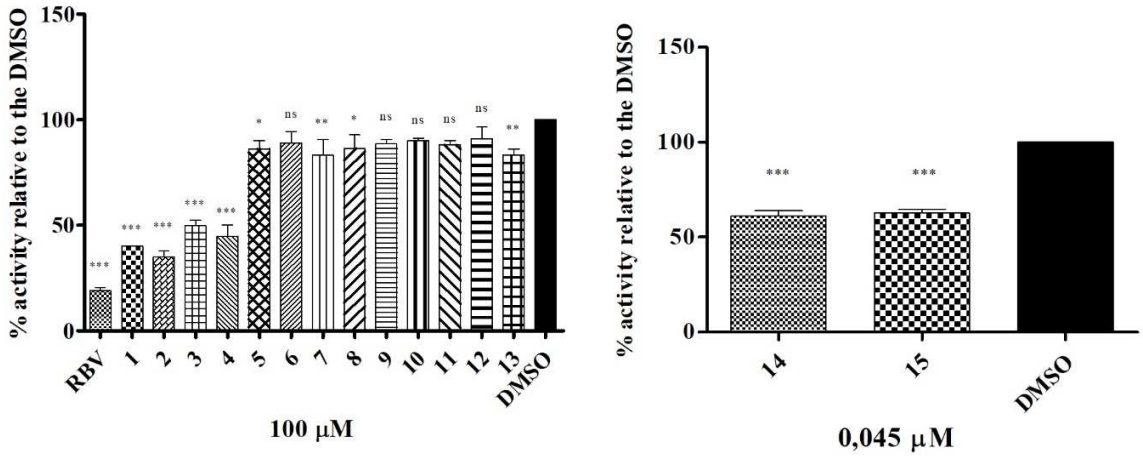

Figure 4. The activity of *C*-nucleoside analogues of RBV on HCVcc replication. Huh 7-J20 cells were inoculated with HCVcc - genotype 2a (JFH-AM71) at an MOI of 0.01. At 2 h post-infection (p.i.) the virus inoculum was removed, cells were washed and treated with DMSO or tested compounds at a dose of 100 µM (1-13) or 0,045 µM (14 and 15). At 72 h p.i., the cell culture medium was collected, and SEAP assay was performed to measure the level of HCVcc replication. Mean absorbance values were expressed as the percentage in comparison to the mean absorbance values detected in DMSO-treated infected cells set as 100%. Error bars represent standard deviations from 3 separate experiments. *: $p \leq 0.05$, **: $p \leq 0.01$, ***: $p < 0.001$, ns:

non-significant compared to infected DMSO-treated cells by one-way ANOVA with Dunnett's post-test.

We further evaluated the antiviral activity of four selected compounds and **RBV** in a dose-response assay. Again, the experiments were conducted using SEAP reporter assay to measure

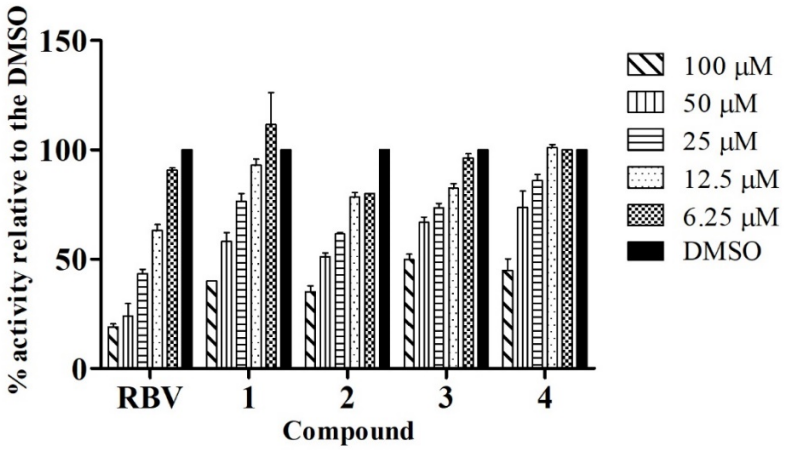

the replication inhibition after treatment with a range of doses (0-100 µM) (Figure 5).

Figure 5. Dose-dependent activity of selected *C*-nucleoside analogues of RBV on HCVcc replication. Huh 7-J20 cells were inoculated with HCVcc - genotype 2a (JFH-AM71) at an MOI of 0.01. At 2 h post-infection (p.i.) the virus inoculum was removed, cells were washed and treated with RBV and tested compounds at the dose range 6.25-100 µM or DMSO. At 72 h p.i., cell culture medium was collected, and SEAP assay was performed to measure the level of HCVcc replication. Mean absorbance values were expressed as the percentage in comparison to the mean absorbance values detected in DMSO-treated infected cells set as 100%. Error bars represent standard deviations from 3 separate experiments.

All tested compounds exhibited the antiviral activity against HCVcc in a dose-dependent manner. The acquired data were used for the estimation of the half-maximal inhibitory concentration value (concentration of a compound that causes a 50% reduction in virus replication, IC_{50}) and selectivity index (SI) defined as the CC_{50}/IC_{50} ratio. The lowest IC_{50} value

of 49.09 μM was estimated for compound **2**, which was over two-times higher than for **RBV** (21.78 μM). Other tested compounds (**1**, **3** and **4**) demonstrated higher IC_{50} values. Due to different toxicity, the calculated SI values for compounds **1**, **2** and **4** were similar (13.4 – 16.8), but still around 3 times lower than for **RBV** (46.8) (Table 2).

Table 2. The antiviral activity of selected compounds against HCVcc virus in comparison to **RBV**.

Compounds	CC_{50} [μM][a]	IC_{50} [μM][b]	SI[c]
RBV	1019.7	21.78	46.8
1	1079.3	68.02	15.7
2	823.13	49.09	16.8
3	730.45	100.5	7.3
4	911.79	68.02	13.4

[a] the half maximal cytotoxic concentration value (CC_{50}), μM

[b] the half-maximal inhibitory concentration value (IC_{50}), μM

[c] the selectivity index - CC_{50}/IC_{50*}

2.2.2. Antiviral activity of *C*-nucleoside analogues of **RBV** against Zika virus

Furthermore, due to the fact that **RBV** was shown to inhibit ZIKV replication in mice,[29] we decided to examine the antiviral activities of all synthesized compounds also against this virus. The cytotoxicity of synthesized compounds has been assessed using the same MTS test used in the previous experiments with HCV. Two cell line models permissive to Zika virus have been chosen: Vero cell line (African green monkey kidney cell line) as it is often considered as a standard cell line for ZIKV assays and Huh 7.5 cell line (Human hepatocellular carcinoma 7.5 cell line) which is often used in anti-flaviviral activity research. [30,31] Again, the CC_{50} values for each compound and **RBV** were determined (Table 3). Compounds **1-13** showed very low cytotoxicity in both cell lines. Within this group of compounds, compound **4** was the most toxic

in both cell lines (CC_{50}: Vero - 597.6 µM, Huh 7.5 – 553.6 µM), however CC_{50} values were still only 2-3 times lower than for **RBV**, depending on the cell line. Again compounds **14** and **15** were relatively toxic with the CC_{50} values estimated on the level of 0.08 and 0.09 µM depending on the cell line.

Table 3. Cytotoxicity of *C*-nucleoside analogues of **RBV** in Vero and Huh 7.5 cell lines.

COMPOUNDS	**CC_{50} [µM][a]**		**COMPOUNDS**	**CC_{50}[µM][a]**	
	Vero	**Huh 7.5**		**Vero**	**Huh 7.5**
RBV	1245.0	1654.0	**8**	1035.0	1023.0
1	1045.0	1919.0	**9**	881.1	907.1
2	967.6	889.6	**10**	649.8	741.9
3	734.5	734.5	**11**	982.8	1088.0
4	597.6	553.6	**12**	713.4	812.2
5	886.4	813.5	**13**	738.9	785.7
6	886.1	834.7	**14**	0.08	0.09
7	1521.0	1598.0	**15**	0.09	0.08

[a] Concentration of the compound needed for 50% reduction in cell viability.

The antiviral activity screening of all synthesized compounds was performed in both cell lines using H/PAN/2016/BEI-259634 Zika virus strain. The nontoxic dose of 100 µM was chosen for compounds **1-13** and 0,045 µM for compounds **14** and **15**. The ELISA assay measuring the level of the ZIKV E glycoprotein in infected and compound treated cells has been utilized to assess the inhibition of virus replication cycle (Figure 6). The screening results showed that compound **2** was the most active in both cell lines. It inhibited the ZIKV virus replication at the level comparable to **RBV** (~80-90%). The calculated IC_{50} values were 33.2 and

37.3 µM for Vero and Huh 7.5 cell, respectively, which led to SI values of 29.1 and 23.8, respectively. The high antiviral activity of this compound against ZIKV confirmed the results obtained for HCV. The rest of tested compounds did not demonstrate significant antiviral activity. In the Vero cell line compound **1** and **4** showed 30-20% inhibition of the ZIKV replication at the dose of 100 µM. However, this effect was not observed in the Huh 7.5 cell line, in which two other compounds **3** and **10** demonstrated stronger activity. Due to the weak antiviral activity of these compounds for ZIKV, only compound **2** was chosen for further analysis.

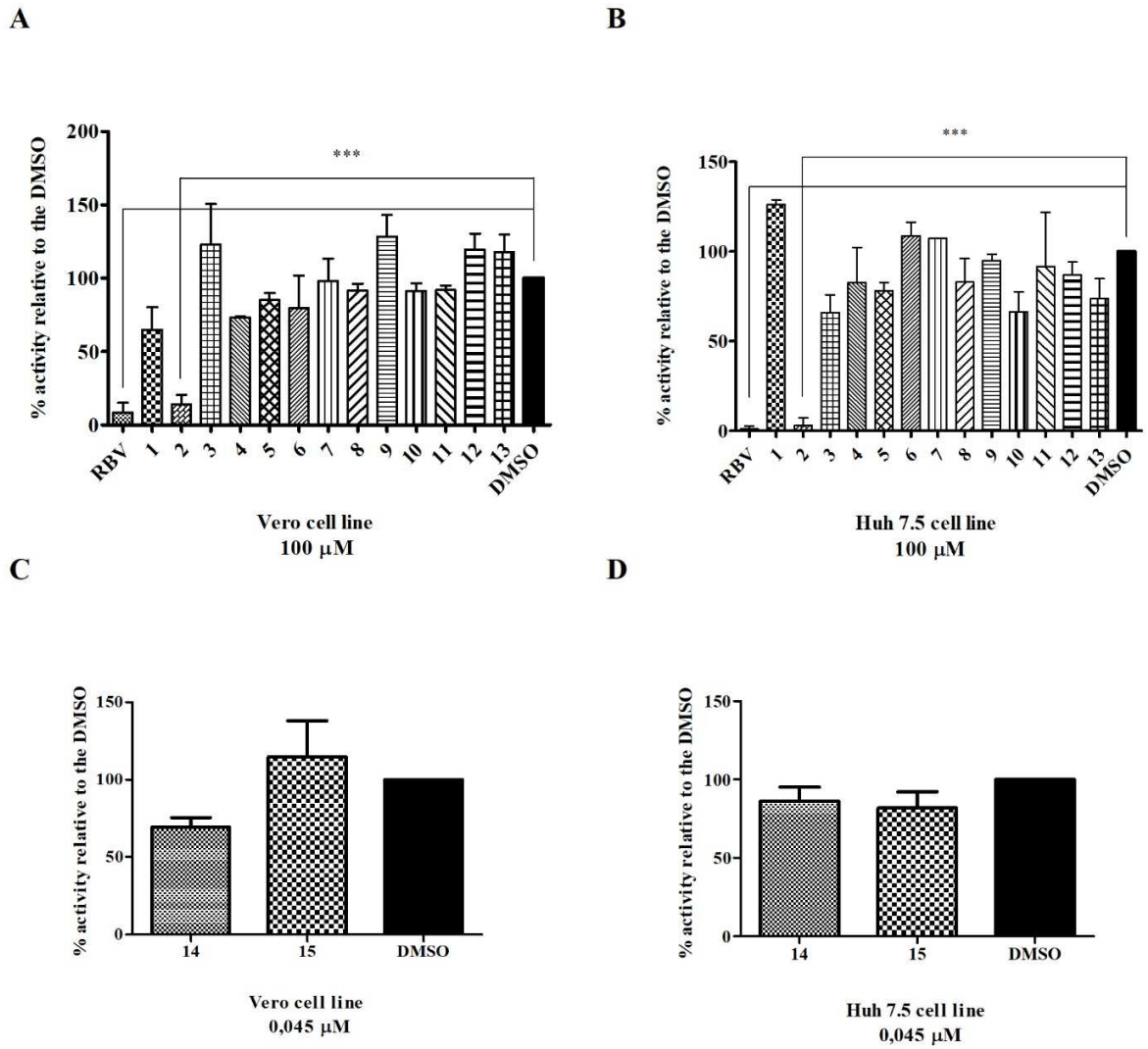

Figure 6. The activity of *C*-nucleoside analogues of RBV on ZIKV infection in two cell line models – Vero (A and C) and Huh 7.5 cell line (B and D). Cells were infected with ZIKV at an MOI of 0.01. At 2 h post-infection (p.i.) the virus inoculum was removed, cells were washed and treated with DMSO, RBV or tested compounds at a dose of 100 µM (1-13) or 0,045 µM (14 and 15). At 72 h p.i., cells were lysed and used for sandwich ELISA assay to measure the level of the ZIKV E glycoprotein. Mean absorbance values were expressed as a percentage in comparison to the mean absorbance values detected in DMSO-treated infected cells set as 100%. Error bars represent standard deviations from 3 separate experiments. ***: $p < 0.001$ compared to infected DMSO-treated cells by one-way ANOVA with Dunnett's post-test.

Compound **2** was further evaluated in a dose-response assay. The decreasing concentrations, starting from 100 µM were tested for the inhibition of virus replication by titration of the released progeny virus particles. Both cell lines were infected with Zika virus at an MOI of 0.01 and treated with compound **2** for 3 days. The cell culture medium was collected, and the infectious virus progeny was titrated using a plaque assay. The dose-dependent antiviral activity of compound **2** was observed in both cell lines represented by the significant dose-dependent manner reduction in viral titers (Figure 7). 90-70% reduction in the virus yield was observed when infected cells were treated with 100-50 µM of the compound.

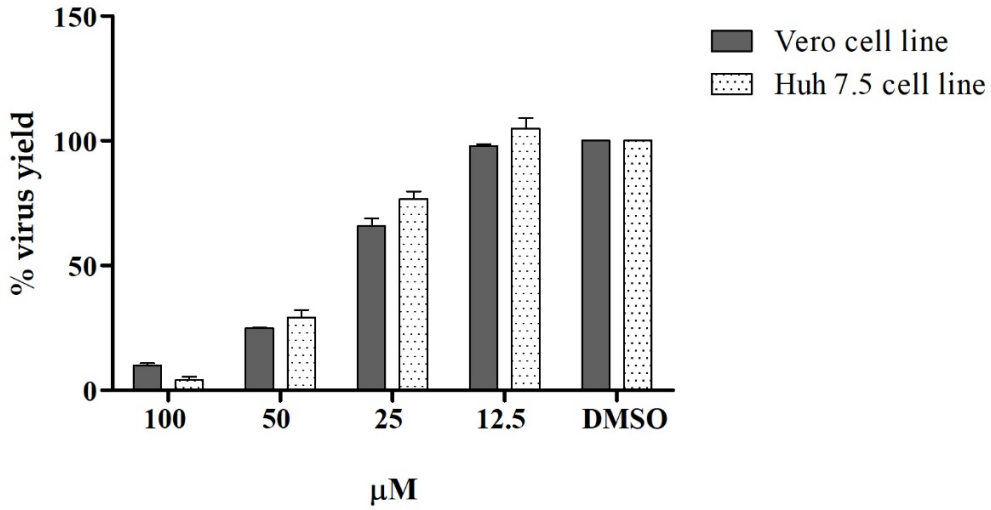

Figure 7. The effect of the compound 2 on Zika virus titers. Vero or Huh 7.5 cells were infected with ZIKV at an MOI of 0.01 and treated with various concentrations of tested

compound (0–100 µM). At 72 h p.i., the culture supernatants were collected to determine virus titers by plaque assay. The virus yield was calculated as percentage in comparison to DMSO-treated infected cells. Error bars represent standard deviations from 3 separate experiments.

This above analysis was used for estimation of half-maximal inhibitory concentration value and selectivity index (Table 4). The same values were determined also for **RBV** in comparison. In Vero cell line IC_{50} values for **RBV** and compound **2** were comparable. In Huh 7.5 cell line the IC_{50} values for compound **2** reached similar level like in Vero cell line, however it was over six times higher than for **RBV**. At this stage it is important to mention the presence of the N-hydroxy-carboxamide group, which seems to be a pharmacophore of interest since it is found in molnupiravir, β-D-N4-hydroxycytidine, the only antiviral marketed against Covid-19 nowadays.[32]

Table 4. The antiviral activity of compound **2** against Zika virus in comparison to **RBV**.

	Vero cell line			Huh 7.5 cell line		
Compounds	**CC_{50} [µM][a]**	**IC_{50} [µM][b]**	**SI[c]**	**CC_{50} [µM][a]**	**IC_{50} [µM][b]**	**SI[c]**
RBV	1245.0	29.9	41.6	1654.0	6.9	239.7
2	967.6	33.2	29.1	889.6	37.3	23.8

[a] the half maximal cytotoxic concentration value (CC_{50}), µM

[b] the half-maximal inhibitory concentration value (IC_{50}), µM

[c] the selectivity index - CC_{50}/IC_{50}

Finally, in order to rationalize our results, we attempted to correlate inhibitory activities as a function of pharmacological parameters, commonly considered in the rules of Lipinsky. These data are presented in Table 5 and unfortunately it is not possible to define a trend relating a parameter like lipophilicity, polarity or the ability to establish hydrogen bonds with the biological activities for the *C*-nucleosides. Further investigations, such as docking, will be undertaken, considering the **RBV** several known targets.

Table 5. Pharmacological parameters [a]

Compound	TPSA °A^2	cLogP	H-bond acceptors	H-bond donors
1	154.48	-2.2	7	5
2	160.82	-2.32	8	6
3	140.59	-1.15	7	5
4	160.82	-1.9	8	6
5	177.89	-2.49	9	6
6	131.81	-1.16	7	4
7	160.82	-0.69	8	6
10	172.79	-0.75	10	2
11	132.58	-0.89	7	3
12	186.67	-1.32	9	5
RBV	143.72	-2.18	7	4

[a] Parameters calculated using swissADME program http://www.swissadme.ch/

3. Conclusions

In this work, we have prepared three new prodrugs and considered modified **SRO-91** compounds as anti-HCV and anti-ZIKV inhibitors. One is the galactosylated *C*-nucleoside to aid in the liver vectorization and two other ones are peptide conjugates with well-described membranotropic properties. Compounds **1-12** have been synthesized previously by functional derivatization of the **SRO-91** carboxamide group. Each synthesized compound was evaluated for broad-spectrum antiviral activity against two single-stranded RNA viruses of the *Flaviviridae* family: hepatitis C virus and Zika virus. Viruses of the *Flaviviridae* family are often associated with human diseases of great medical importance; with HCV and ZIKV as examples. Although extensive research has been carried out in many laboratories, no vaccine or treatment have been approved for clinical use against ZIKV, and the multidrug therapy available for HCV will need to be improved in the future as drug-resistant strains will emerge.

The biological evaluation of anti-HCV activity was done using HCVcc system in Huh 7-J20 reporter cell line. Four compounds: **1, 2, 3, 4** demonstrated strong inhibition of the HCVcc replication (IC_{50} 49.1-100.5 µM) despite their pharmacological profile is not completely in accordance with expected properties with a polarity and a high solubility in water (Table 2). The highest activity was shown by compound **2** (IC_{50} 49.09 µM; SI 16.8) bearing the most acidic functionality (hydroxamic acid), which certainly helps in the formation of hydrogen bonds.

However, the antiviral activity was still lower than that caused by **RBV** (IC_{50} 21.78 μM; SI 46.8).

Furthermore, we have examined the antiviral activity of all studied compounds against Zika virus in two cell line models: Vero and Huh 7.5 cell lines. Previously, it was shown that the activity of **RBV** varied between cell lines derived from different hosts.[33] Some of the synthesized compounds examined by us showed variable activity in tested cell lines – *e.g.,* compound **1** demonstrated weak activity in Vero cell line, but was not active in Huh 7.5 cell line. Only, compound **2** exhibited high antiviral activity against Zika virus in two cell lines (Vero and Huh 7.5 cell lines). Together with strong anti-HCV activity it confirms its broad-spectrum antiviral activity with acceptable selectivity indexes. It is worth pointing out that compound **2** inhibited ZIKV replication at the level comparable to **RBV** (~ 80-90% at the dose of 100 μM). In both cell line, a dose-dependent effect was observed for this compound. The calculated IC_{50} value of 33.2 μM was calculated for Vero cell line and 37.3 μM for Huh 7.5 cell line. Due to the low cytotoxicity of this compound, the SI values were estimated on the level of 23.8-29.1.

The synthesized prodrugs were supposed to improve lipophilic properties (compound **12**) and the uptake of the compounds by the cells (compound **14** and **15**), as well as its targeting to hepatic cells (compound **13**), which overall should increase the antiviral activity. Unfortunately, introduced modifications to the compound **1** did not changed the activity of the compounds as expected. Compounds **12** and **13** were depleted for anti-HCV activity as compared to compound **1** and the activities of compounds **14** and **15** were slightly lower along with toxicity. In case of ZIKV, weak activities were observed for compound **13** in Huh 7.5 cell line and compound **14** in Vero cell line. The weak activity of compound **13** could be caused by the relatively low expression of galactosides receptors on Huh 7.5 cells. Oh *et al.* group has used the Huh 7 cell line in the examination of galactosylated liposomes, but other study shows relatively low density of ASGP-R receptor on the Huh 5-2 cell line, as compared to HepG2 cell line.[34,35] Thus, it would be noteworthy to examine the biological activity of compound **13** in another hepatic cell line, with confirmed ASGP-R expression.

Overall, our data showed that compound **2** possesses moderate *in vitro* antiviral activity against two members of the *Flaviviridae* family. However, new derivatives of this compound can be synthesized to improve its antiviral potential.

4. Experimental

4.1.Chemistry

All reactions were conducted under an inert atmosphere of argon. Metallic indium was purchased from Alfa Aesar. Dichloromethane was distilled under argon over CaH_2. ^1H and ^{13}C NMR spectra were recorded in $CDCl_3$ or CD_3OD on a Jeol 400 MHz ECX. High resolution mass spectra were obtained with a LTQ orbitrap spectrometer. Optical rotations were determined at 25 °C in $CHCl_3$ or MeOH, 589 nm, on an Anton Paar MCP200 instrument and IR spectra were recorded on a Bruker Tensor 27 spectrophotometer. Thin layer chromatography was carried out on silica gel plates (Macherey-Nagel), spots were detected with UV light and revealed with H_2SO_4 solution. Flash chromatography was performed with silica gel 60, 40-63 µm.

Complete synthetic procedures and characterization of intermediates are provided in the Supporting Information.

*2',3',5'-Tri-O-acetyl-5-(β-D-ribofuranosyl)-2H-1,2,3-triazole-4-carboxamide (**10**)*

Compound **1 SRO-91** (80 mg, 0.33 mmol) was stirred at room temperature in acetic anhydride (1 mL) and pyridine (1 mL) overnight. The reaction was quenched with methanol and the solvent evaporated under vacuum. The crude was purified by flash column chromatography on silica gel (cyclohexane/ethyl acetate: 1/1) affording **11** as a white solid (115 mg, 94%). ^1H NMR (400 MHz, $CDCl_3$) δ 7.28 (s, 1H, NH), 6.50 (s, 1H, NH), 5.70 (d, *J* = 4.4 Hz, 1H, $H_{1'}$), 5.64 (dd, *J* = 4.8, 4.8 Hz, $H_{2'}$), 5.35 (dd, *J* = 5.7, 5.7 Hz, $H_{3'}$), 4.33 (m, 2H, $H_{4'}$, $H_{5'}$), 4.24 (dd, *J* = 12.7, 6.4 Hz, $H_{5'}$), 2.05 (s, 6H, CH_3CO), 2.03 (s, 3H, CH_3CO). ^{13}C NMR (100 MHz, $CDCl_3$) δ 171.5 ($COCH_3$), 170.1 ($COCH_3$), 170.0 ($COCH_3$), 162.9 ($CONH_2$), 143.4 (C_5), 138.2 (C_4), 79.2 ($C_{4'}$), 75.3 ($C_{1'}$), 74.4 ($C_{2'}$), 71.5 ($C_{3'}$), 63.8 ($C_{5'}$), 20.9 (CH_3CO), 20.7 (CH_3CO). HRMS (ESI) calcd for $C_{14}H_{19}N_4O_8$ $[M+H]^+$: 371.1203; found: 371.1196.

1-(5-carbamoyl-2H-1,2,3-triazol-4-yl)-1,5-dideoxy-β-D-ribofuranos-5-yl 6-aminohexanoate *(**12**)*

To a solution of compound **21** (500 mg, 0.8 mmol) in ethanol (10 mL) was added palladium chloride (57 mg, 0.4 mmol). The reaction mixture was hydrogenated at room temperature for 72 h under 4 bars. The reaction mixture was filtered through Celite® and washed with ethanol. The solvent was removed under reduced pressure and the residue was purified by flash column

chromatography (cyclohexane/ethyl acetate: 1/4 to methanol/ethyl acetate 1/1) to afford 4-(5'-O-(6-aminohexanoyl)-β-D-ribofuranosyl)-2H-1,2,3-triazole-5-carboxamide **12** (113 mg, 40%) as a white sticky solid. $[\alpha]_D^{25}$ +9.8 (MeOH, *c* 0.7). ^{1}H NMR (400 MHz, CD_3OD) δ 5.44 (d, *J* = 4.8 Hz, 1H, $H_{1'}$), 4.39 (dd, *J* = 11.5, 2.7 Hz, 1H, $H_{5'}$), 4.33 (t, *J* = 4.7 Hz, 1H, $H_{2'}$),), 4.23 (dd, *J* = 11.6, 5.3 Hz, 1H, $H_{5'}$), 4.19-4.12 (m, 2H, $H_{3'}$, $H_{4'}$), 2.91 (t *J* = 7.6 Hz, 2H, H_6), 2.35 (t, *J* = 7.3 Hz, 2H, H_2), 1.71–1.55 (m, 4H, H_3, H_5), 1.46-1.33 (m, 2H, H_4). ^{13}C NMR (100 MHz, CD_3OD) δ 174.9 (OCO), 165.3 ($CONH_2$), 144.9 (C_4 triazole), 139.1 (C_5 triazole), 83.0 ($C_{4'}$), 78.7 ($C_{1'}$), 76.7 ($C_{2'}$), 73.4 ($C_{3'}$), 65.6 ($C_{5'}$), 40.6 (C_6), 34.5 (C_2), 28.2 (C_5), 26.8 (C_4), 25.3 (C_3). HRMS (ESI) calcd for $C_{14}H_{24}N_5O_6$ $[M+H]^+$: 358.1727; found: 358.1719.

*2-[2-(2-ethoxy)ethoxy]ethyl-β-D-galactopyranosyl1-(5'-carboxamyl-2',3',4'-triazole)-β-D-ribofuranosyl succinate **(13)***

To a mixture of **30** (66 mg, 56 µmol) and EtOH (3 mL), Pd on charcoal (12 mg, 20% mol) is added. The resulting mixture is poured into a Parr bomb and left under stirring and H_2 (8 bars) for 2 days. Pd/C (5 mg, 10% mol) is then added and the mixture is left for another 3 days under stirring. The reaction mixture is filtered on Celite®, rinsed with EtOH and concentrated under reduced pressure. The crude is finally purifier on silica gel (dichloromethane/methanol 7/3) yielding **13** (15 mg, 40%) as a white solid. $[\alpha]_D^{20}$ +7 (CH_3OH, *c* 0.5). ^{1}H NMR (400 MHz, CD_3OD) δ 5.44 (d, *J* = 4.8 Hz, 1H, $H_{1''}$), 4.40 (dd, *J* = 2.8 Hz, 11.8 Hz, 1H, $H_{5''}$), 4.43 - 4.12 (m, 5H, H_1, $H_{2''}$, $H_{3''}$, $H_{4''}$, and $H_{5''}$), 4.05 - 3.99 (m, 1H, $H_{1'}$), 3.83 (d, *J* = 2.9 Hz, 1H, H_4), 3.76 - 3.43 (m, 16H, H_2, H_3, H_5, H_6, $H_{1'}$, $H_{2'}$, $H_{3'}$, $H_{4'}$, $H_{5'}$ and $H_{6'}$), 2.68-2.58 (m, 4H, $H_{7'}$ and $H_{8'}$). ^{13}C NMR (100 MHz, $CDCl_3$) δ 174.30, 174.08 (-COOC), 165.53 ($C_{8''}$), 144.76, 139.12 ($C_{6''}$ and $C_{7''}$), 105.11 (C_1), 83.24 ($C_{4''}$), 78.77, 76.96, 76.81, 74.98, 73.33, 72.64 (C_2, C_4, C_5, $C_{1''}$, $C_{2''}$ and $C_{3''}$) 71.56, 71.53, ($C_{1'}$ and $C_{6'}$) 70.46 (C_3), 70.18, 69.72, 65.83, 65.09, 62.66 (C_6, $C_{2'}$, $C_{3'}$, $C_{4'}$ and $C_{5''}$), 30.02 ($C_{7'}$ and $C_{8'}$). HRMS (ESI) calcd for $C_{24}H_{39}N_4O_{16}$ $[M+H]^+$: 639.2356; found = 639.2351

Peptide synthesis

Peptide syntheses were performed using standard Fmoc-based solid phase synthesis (SPPS) with a Liberty Blue automated microwave synthesizer (CEM Corporation, Matthews, NC, USA). The resin used was a Fmoc-Rink-amide NovaSyn TGR resin (loading 0.48 mmol/g). Standard

Fmoc-protected amino acids were coupled using 5 eq, DIC (5 eq) and Oxyma pure (5 eq) in DMF, assisted by microwaves (75°C and 170 W for 17s followed by 90°C and 30 W for 110s). Fmoc removal was achieved using a 20% piperidine solution in DMF assisted by microwaves (75°C and 155W for 15s, performed twice). More specifically, Arg residues were coupled using a double coupling procedure composed of two steps of 1500s at 25°C without microwaves followed by 120s at 75°C assisted by microwaves (30 W). His residues were coupled via a single coupling procedure composed of two steps of 120s at 25°C without microwaves followed by 480s at 50°C assisted by microwaves (35 W). The pegylation was performed by manual SPPS using Fmoc-TTDS-OH (2.5 eq), TBTU (2.5 eq) and DIPEA (3.5 eq) in DMF for 30 min at room temperature. The nucleoside 5-[2',3'-*O*-isopropylidene-5'-*O*-(3''-carboxy-1''-oxopropyl)-β-D-ribofuranosyl]-2*H*-1,2,3-triazole-4-carboxamide **25** (2.5 eq) was coupled manually using TBTU (2.5 eq) and DIPEA (3.5 eq) in DMF for 30 min at room temperature.

After sequence elongation, the peptides were deprotected and cleaved from the resin by treatment with a cleavage cocktail composed of TFA/H_2O/Phenol/TIS (90:5:3:2) for 4h at room temperature. The resulting cleavage mixture were filtered and evaporated under air flush. The crude peptide was then precipitated in cold diethyl ether, centrifugated, dissolved in mQ water and lyophilized overnight.

The crude peptides were finally purified by semi-preparative RP-HPLC using a mixture of mQ water containing 0.1% TFA (solvent A) and CH_3CN containing 0.1% TFA (solvent B), on a Phenomenex Jupiter C18 (250 mm×4.6 mm) column. HPLC-MS analyses were performed on a Alliance Chromatography (Waters) apparatus with a Phenomenex Kinetex C18 column (2.6 µm, 3.0 x 100 mm) using a mixture of mQ water containing 0.1% TFA (solvent A) and CH_3CN containing 0.1% TFA (solvent B) at 0.6 mL/min.

Conjugate 14

Conjugate **14** was synthesized on a 0.05 mmol scale by SPPS using Fmoc/tBu strategy, as described above. The crude peptide was purified using a 15-30% B in A gradient in 30 min. The peptide was obtained as a white powder (60.3 mg; 55 %) in purity ≥ 95 % ($[M+3H]^{3+}$: 759.91 Da ; rt: 4.03 min by RP-HPLC ESI-MS with a 15-60% B eluent in 5 min).

Conjugate 15

Conjugate **15** was synthesized on a 0.05 mmol scale by SPPS using Fmoc/tBu strategy, as described above

The crude peptide was purified using a 20-35% B in A gradient in 30 min. The peptide was obtained as a white powder (8.5 mg ; 12 %) in purity ≥ 95 % ($[M+2H]^{2+}$: 1121.78 Da ; rt: 4.08 min by RP-HPLC ESI-MS with a 20-35% B eluent in 5 min).

4.2. Biology

Compounds

The synthesized compounds were dissolved in DMSO at a concentration of 20 mg/ml and stored at −20°C.

Cells and viruses

The Vero cell line (African green monkey kidney cell line) and Huh 7.5 (human hepatocellular carcinoma 7.5 cell line) were cultured in Dulbecco's Modified Eagle's Medium (D-MEM) (Corning, New York, USA) supplemented with 8% heat-inactivated fetal bovine serum (FBS), 100 U/mL penicillin, and 100 g/mL streptomycin at 37 °C under 5% CO_2. Huh 7-J20 cell line was cultured with supplementation of puromycin (2 µg/mL) and nonessential amino acids. Zika virus strain - ZIKV H/PAN/2016/BEI-259634) was cultured in Vero cells for 3–4 days and the viral titer was determined using a plaque assay.

HCVcc virus was generated in the Huh-7.5 cell culture as previously described.[32] Briefly, the pUC-JFH-1/AM71 plasmid was linearized using Xba I, purified by a clean-up kit (Qiagen, Hombrechtikon, Switzerland), and further used for transcription using the TranscriptAid T7 High Yield Transcription Kit according to the manufacturer's protocol. Isolated genomic RNA was used for electroporation of Huh-7.5 cells. 72 h post electroporation cell culture medium containing HCVcc was collected, filtered and aliquoted. $TCID_{50}$/ml titer of HCVcc was determined by using a pseudo-plaque assay. Huh-7.5 cells seeded in a 96-well plate were infected with serial dilutions of HCVcc stock for 3 h. The virus was removed, fresh medium was

added for 72 h and then immunoperoxidase monolayer assay was performed to detect pseudo-plaques. Cells were fixed with cold methanol, permeabilized in 0.5% Triton X-100 in PBS for 10 min. After washing, cells were incubated with HCV anti-core antibody (Hep C cAg antibody (C7-50); 1:300 dilution) for 1 h followed by incubation with anti-mouse HRP-labelled secondary antibody (1:1000 dilution) for another 1 h. HCV pseudo-plaques were stained using a Vector Nova Red kit and counted.

Cell viability assay

Compounds cytotoxicity was determined using the CellTiter 96 AQueous non-radioactive cell proliferation assay (MTS) according to the manufacturer's instructions. The analysis was done in three replicates. The half-maximal cytotoxic concentration (CC_{50}) values of compounds that reduce the cell viability in 50% were calculated using the GraphPad Prism software (version 5.01) from the dose–response curves.

SEAP assay

Subconfluent cultures of Huh 7-J20 cells were infected with HCVcc (MOI 0.01) and treated for 72 h with various concentrations of synthesized compounds, DMSO or ribavirin. The level of HCV replication was determined by the secreted alkaline phosphatase (SEAP) activity quantification using Phospha-Light™ SEAP Reporter Gene Assay System according to the manufacturer's instructions with minor modifications. 50 µL of culture medium was mixed with 50 µL of assay buffer and incubated for 7 min at room temp. Next, 50 µL of substrate was added, incubated for 45 min, and the SEAP level was read in a luminescence multi-well scanner. IC_{50} values were calculated using GraphPad Prism software.

Anti-ZIKV activity screening of compounds

Vero or Huh 7.5 cells were seeded a day before infection. Cells were infected with the ZIKV H/PAN/2016/BEI-259634) at an MOI of 0.01. At 2 h post-infection (p.i.) the virus inoculum was removed, cells were washed and treated with DMSO or tested compounds at dose of 100 µM (1-15) or 0,0003 µM (16 and 17). At day 3 post infection, cells were lysed in lysis buffer (20 mM Tris-HCl pH 7.4, 20 mM iodoacetamide, 150 mM NaCl, 1 mM EDTA, 0.5% Triton X-100 and Complete™ protease inhibitors) and the E protein level was assessed by sandwich ELISA assay.

Sandwich ELISA assay

MICROLON® 96W Microplate 96-well plates were coated with pan-flavivirus anti-E MAb D1-4G2-4-15(4G2) (Absolute antibody) in PBS. The antibody was removed, and the wells were blocked for 2 h at room temperature (RT) with 3% BSA in PBS containing 0.02% Tween-20 (PBS-T). After washing with PBS-T, cell lysates were added and incubated for 2 h at RT. Wells were washed with PBS-T and incubated with anti-E rabbit R34 antibody (kind gift from Dr Arvind Patel, MRC, University of Glasgow Centre for Virus Research, University of Glasgow, Glasgow, UK) at 6 µg/ml in PBS-T for 1 h at RT. Plates were washed again and the secondary antibody - anti-rabbit HRP conjugate were added for 1 h at RT. Next, TMB substrate was added and the reaction was stopped with 0,5M H_2SO_4. Absorbance at 450 nm was measured in a microplate reader.

Dose-response assay

Vero or Huh 7.5 cells were infected with Zika virus (MOI 0.01) and treated with increasing doses of tested compound (0 to 100 µM). Culture media were collected 3 days post-infection and further used for the determination of ZIKV titers using the plaque assay. The dose–response curves were modeled using GraphPad Prism software and used for calculations of the half-maximal inhibitory concentration (IC_{50}) values, indicating the dose required to reduce the viral yield by 50% compared to the non-treated infected cells.

Plaque assay

Confluent cultures of Vero cells were inoculated with 10-fold dilutions of collected culture media for 2 h at 37°C. Then, cells were overlaid with 1% carboxymethylcellulose in Dulbecco's Modified Eagle's Medium (DMEM). After 4 days the medium was removed, the cells were washed with PBS and stained with the solution of 0.5% crystal violet to count the plaques and calculate the virus titers (PFU/ml).

Statistical analysis

All statistical analyses were performed using GraphPad Prism version 5.01. Error bars are expressed as ± SD. One-way ANOVA analysis with Dunnet's post-test was performed to

compare the results of the antiviral activity screening of the compounds. P values of < 0.001 were considered significant.

Acknowledgement: The following reagent was obtained through BEI Resources, NIAID, NIH: Zika Virus, H/PAN/2016/BEI-259634, NR-50210

Funding Sources

This work was funded by The National Centre for Research and Development, Poland, grant number LIDER/1/0031/L-7/15/NCBR/2016 and the National Science Centre, Poland, grant number UMO-2011/03/N/NZ6/00059.

References

- [1] Pushpakom S, Iorio F, Eyers PA, Escott KJ, Hopper S, Wells A, Doig A, Guilliams T, Latimer J, McNamee C, Norris A, Sanseau P, Cavalla D, Pirmohamed M, Drug Repurposing: Progress, Challenges and Recommendations, *Nat. Rev. Drug Discov.* 2019; 41-58.

[2] https://clinicaltrials.gov/ct2/show/NCT01056523

- [3] Borden KLB, Culjkovic-Kraljacic B. Ribavirin as an anti-cancer therapy: acute mueloid leukemia and beyond? *Leuk. Lymphoma* 2010; 51: 1805-1815.

[4] Gong Y, Shi F. The anti-leukemia role and mechanism of ribavirin in Ph+ leukemia, Blood 2014; 124: 5278.

[5] Casaos J, Gorelick NL, Huq S, Choi J, Xia Y, Serra R, Felder R, Lott T, Kast RE, Suk I, Brem H, Tyler B, Skuli N. The use of ribavirin as an anticancer therapeutic: will it go viral? *Mol. Cancer Ther*. 2019; 18: 1185-94.

[6] https://www.clinicaltrialsregister.eu/ctr-search/search?query=Ribavirin+(RBV)&page=1

[7] Liu C, Zhou Q, Li Y, Garner L.V, Watkins S P, Carter L J, Smoot J, Gregg A.C, Daniels A D, Jervey S, Albaiu D. Research and development on therapeutic agents and vaccines for COVID-19 and related human coronavirus diseases, *ACS Cent. Sci.* 2020; 6: 315-331.

[8] Wambecke A, Laurent-Issartel C, Leroy-Dudal J, Giffard F, Cosson F, Lubin-Germain N, Uziel J, Kellouche S, Carreiras F. Evaluation of the potential of a new ribavirin analog impairing the dissemination of ovarian cancer cells, *PLoSONE* 2019; 14: e0225860.

- [9] Sabat N, Migianu-Griffoni E, Tudela T, Lecouvey M, Kellouche S, Carreiras F, Gallier F, Uziel J, Lubin-Germain N. Synthesis and antitumor activities investigation of a *C*-nucleoside analogue of Ribavirin, *Eur. J. Med. Chem.* 2020; 188: 112009.

[10] Beaucourt S, Vignuzzi M. Ribavirin: a drug active against many viruses with multiple effects on virus replication and propagation. Molecular basis of ribavirin resistance, *Curr Opin Virol*. 2014; 8: 10-15.

[11] a) Pardo, J.; Shukla, A. M.; Chamarthi, G.; Gupte, A. Drugs in Context **2020**, *9*, 1. b) Reza Hashemian, S. M.; Farhadi, T.; Velayati, A. A. Drug Design, Development and Therapy **2020**, *14*, 3215.

[12] De Clercq E. *C*-Nucleosides to be revised, *J. Med. Chem.* 2016; 59: 2301-2311.

[13] Kharb R, Shahar Yar M, Chander Sharma P. Recent advances and future perspectives of triazole analogs as promising antiviral agents, *Mini-Reviews Med. Chem.* 2011; 11: 84-96.

[14] Sierocki, P.; Gaillard, K.; Reyes, R.A.A.; Donnart, C.; Lambert, E.; Grosse, S.; Arzel, L.; Tessier, A.; Guillemont, J.; Mathé-Allainmat, M.; Lebreton, *J. Org. Biomol. Chem*. **2022**, 20: 2715

[15] Elfiky, A. A. *Life Sciences* **2020**, *253*: 117592.

[16] Manns MP, Buti M, Gane E, Pawlotsky JM, Razavi H, Terrault N, Younossi Z. Hepatitis C virus infection, *Nat Rev Dis Primers* 2017; 3: 17006.

[17] Gorshkov K, Shiryaev SA, Fertel S, Lin YW, Huang CT, Pinto A, Farhy C, Strongin AY, Zheng W, A.V. Terskikh, Zika virus: origins, pathological action, and treatment strategies, *Front Microbiol.* 2019; 9: 3252.

[18] Solarte C, Dos Santos M, Gonzalez S, Miranda LSM, Guillot R, Ferry A, Gallier F, Uziel J, Lubin-Germain N. Synthesis of *C*-ribosyl-1,2,3-triazolyl carboxamides, *Synthesis* 2017; 49: 1993-2002.

[19] Cosson F, Faroux A, Baltaze JP, Farjon J, Guillot R, Uziel J, Lubin-Germain N, Synthesis of ribavirin 2'-Me-*C*-nucleosides analogues, *Beilstein J. Org. Chem.* 2017; 13 :755-761.

[20] Ait Youcef R, Dos Santos M, Roussel S, Baltaze JP, Lubin-Germain N, Uziel J. Huisgen cycloaddition reaction of *C*-alkynyl ribosides under micellar catalysis: synthesis of ribavirin analogues. *J. Org. Chem.* 2009; 74: 4318-4323.

[21] Sabat, N, Ouarti A, Migianu-Griffoni E, Lecouvey M, Ferraris O, Gallier F, Peyrefitte C, Lubin-Germain N, Uziel J. Synthesis, antiviral and antitumor activities investigations of a series of Ribavirin *C*-nucleoside analogue prodrugs. *Bioorganic Chem.* 2022; 122: 105723.

- [22] Tam RC, Ramasamy K, Bard J, Pai B, Lim C, Averett DR. The ribavirin analog ICN 17261 demonstrates reduced toxicity and antiviral effects with retention of both immunomodulatory activity and reduction of hepatitis-induced serum alanine aminotransferase levels, *Antimicrob. Agents Chemother.* 2000; 4: 1276-1283.

[23] Weis AL, Shanmuganathan K, Goodhue CT, L-ribofuranosyl nucleosides, EP1132393A1, US5559101A.

[24] Koff WC, Pratt RD, Elm J, Venkateshan CN, Halstead SB. Treatment of intracranial dengue virus infections in mice with a lipophilic derivative of ribavirin, *Antimicrob. Agents Chemother.* 1983; 24: 134-136.

- [25] Gomes B, Santos NC., Pototto M. Biophysical properties and antiviral activities of meales fusion protein drived peptide conjugated with 25-hydroxycholesterol, *Molecules* 2017; 22: 1869-1884.

[26] Gonzalez S, Gallier F, Kellouche S, Carreiras F, Novellino E, Carotenuto A, Chassaing G, Rovero P, Uziel J, Lubin-Germain N. Studies of membranotropic and fusogenic activity of two putative HCV fusion peptides, *BBA Biomembranes* 2019; 1861: 50-61.

[27] Walrant A, Cardon S, Burlina F, Sagan S. Membrane crossing and membranotropic activity of cell-penetrating peptides: dangerous liaisons? *Acc. Chem. Res.* 2017; 50: 2968-2975.

[28] Iro M, Witteveldt J, Angus AG, Woerz I, Kaul A, Bartenschlager R,Patel AH. A reporter cell line for rapid and sensitive evaluation of hepatitis C virus infectivity and replication, *Antiviral Res.* 2009; 83 : 148-155.

[29] Kamiyama N, Soma R, Hidano S, Watanabe K, Umekita H, Fukuda C, et al. Ribavirin inhibits Zika virus (ZIKV) replication in vitro and suppresses viremia in ZIKV-infected STAT1-deficient mice, *Antiviral Res.* 2017, 146 :1-11.

[30] Mumtaz N, Jimmerson LC, Bushman LR, Kiser JJ, Aron G, et Al.Cell-line dependent antiviral activity of sofosbuvir against Zika virus, *Antiviral Res.* 2017; 146 : 161-163.

[31] Farfan-Morales CN, Cordero-Rivera CD, Osuna-Ramos JF, et al. The antiviral effect of metformin on zika and dengue virus infection, *Sci Rep* 2021; 11: 8743.

[32] Khiali S, khani E, Rouy S.B. Comprehensive review on molnupiravir in COVID-19: a novel promising antiviral to combat the pandemic *Future Microbiology* , **2022**, 17:377-391

[33] Krol E, Wandzik I, Pastuch-Gawolek G, Szewczyk B Anti-hepatitis C virus activity of uridine derivatives of 2-deoxy sugars, *Molecules* 2018; 23: 154.

[34] Franco EJ, Rodriquez JL, Pomeroy JJ, Hanrahan KC, Brown AN. The effectiveness of antiviral agents with broad-spectrum activity against chikungunya virus varies between host cell lines, *Antivir Chem Chemother.* 2018; 26 :1-7.

[35] Oh HR, Jo HY, Park JS, et al. Galactosylated liposomes for targeted co-delivery of doxorubicin/vimentin siRNA to hepatocellular carcinoma, Nanomaterials 2016; 6: 141.

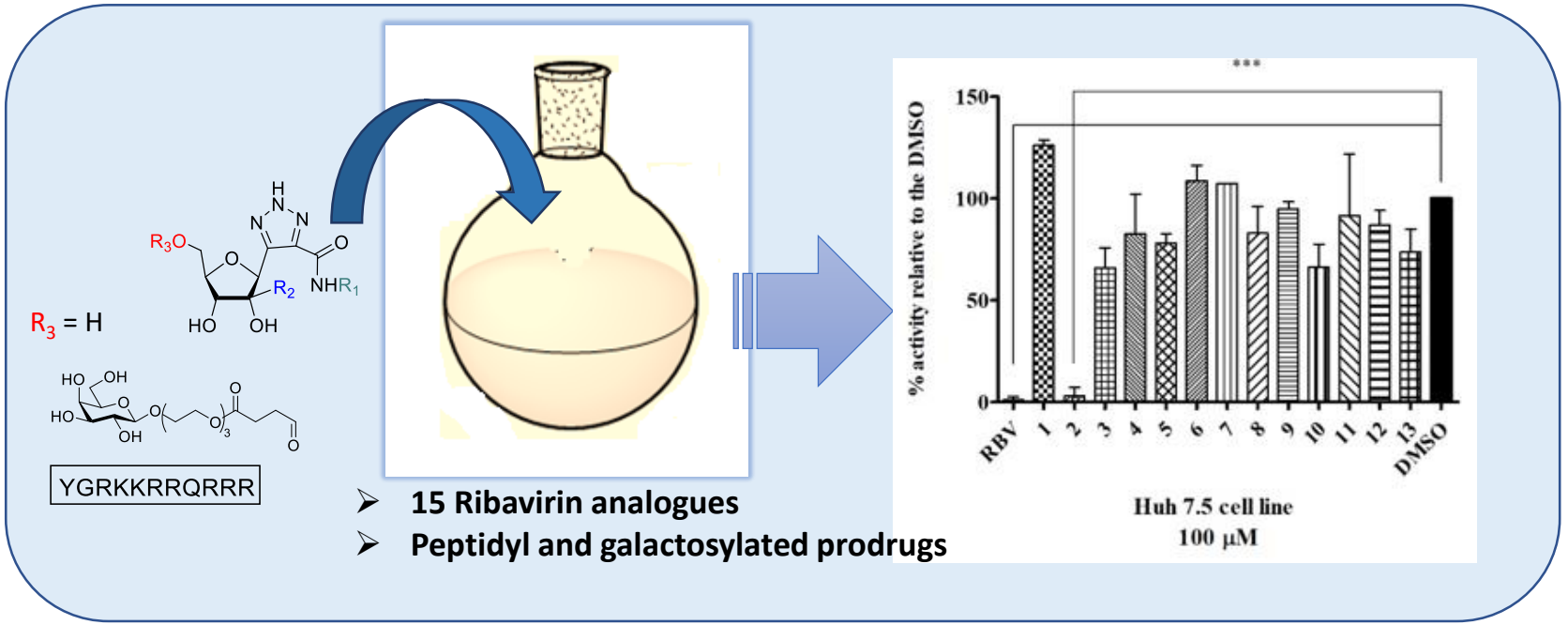
R3O
R2
NHR1
HO
OH
R3 = H
HO
OH
HO
OH
O
O
O
3
O
YGRKKRRQRRR
➢ 15 Ribavirin analogues
➢ Peptidyl and galactosylated prodrugs
***
% activity relative to the DMSO
150
100
50
0
RBV
1
2
3
4
5
6
7
8
9
10
11
12
13
DMSO
Huh 7.5 cell line
100 µM